

Experimental Demonstration of Greenberger-Horne-Zeilinger Correlations Using Nuclear Magnetic Resonance

Richard J. Nelson[†]

David G. Cory^{*}

Seth Lloyd[†]

[†] d'Arbelloff Laboratory for Information Systems and Technology

Department of Mechanical Engineering

^{*} Department of Nuclear Engineering

Massachusetts Institute of Technology

Cambridge, Mass. 02139

Abstract: The Greenberger-Horne-Zeilinger (GHZ) effect provides an example of quantum correlations that cannot be explained by classical local hidden variables. This paper reports on the experimental realization of GHZ correlations using nuclear magnetic resonance (NMR). The NMR experiment differs from the originally proposed GHZ experiment in several ways: it is performed on mixed states rather than pure states; and instead of being widely separated, the spins on which it is performed are all located in the same molecule. As a result, the NMR version of the GHZ experiment cannot entirely rule out classical local hidden variables. It nonetheless provides an unambiguous demonstration of the “paradoxical” GHZ correlations, and shows that any classical hidden variables must communicate by non-standard and previously undetected forces. The NMR demonstration of GHZ correlations shows the power of NMR quantum information processing techniques for demonstrating fundamental effects in quantum mechanics.

Quantum mechanics is well-known to exhibit strange and apparently paradoxical effects. Perhaps the strangest of these effects is the possibility of correlations between quantum-mechanical systems that cannot be explained by appealing to an underlying theory of local hidden variables—classical variables whose unknown or “hidden” states supply the apparent stochastic results to quantum experiments [1, 2, 3, 4, 5, 6]. A striking contradiction with the local hidden variable picture is obtained in the Greenberger-Horne-Zeilinger (GHZ) effect, in which a set of measurements on three correlated quantum particles gives results that are perfectly correlated in a pattern that is classically impossible [7]. This paper reports the first experimental demonstration of GHZ correlations.

GHZ experiments that verify both the “weird” quantum correlations and the non-local nature of physical reality are difficult to realize in the laboratory, where the problems associated with faithfully preparing the required state $|\psi\rangle$ and making the necessary measurements pose formidable obstacles. However, recent discoveries in the field of quantum information processing using NMR make possible an analog GHZ experiment that validates the GHZ correlations required by a quantum mechanical description of the universe [8, 9, 10]. The idea of using NMR to demonstrate GHZ correlations was proposed in [11], and an effective GHZ state was first created using NMR in [12]. NMR offers a number of advantages in performing tests of few-particle quantum mechanics, including: (1) weak measurements that allow the direct determination of ensemble density matrices; (2) long decoherence times; (3) simple, well-understood Hamiltonians; (4) gradient techniques that allow the construction of effective pure states and the controlled decoherence of samples. These features of NMR make it possible to use quantum systems in mixed states at room temperature to mimic precisely the dynamics of a quantum system in a pure state at low temperature. As a result, NMR is an ideal testbed for the predictions of quantum mechanics for few-variable systems.

Despite the advantages of NMR quantum information processing techniques listed above, it is important to note that demonstrating GHZ correlations using NMR differs in significant ways from performing the GHZ experiment as originally envisaged. In particular, because the NMR experiment is inherently local, the NMR demonstration of GHZ correlations cannot rule out nonstandard interactions between classical hidden variables that conspire to exhibit apparently quantum mechanical correlations. In addition, because the NMR experiment is performed on thermal states, though the spins in the experiment mimic the effects of entanglement, they are not in fact entangled: as a result, the NMR experiment cannot rule out local hidden variables. Nonetheless, the NMR demonstration of GHZ correlations provides an unambiguous and statistically significant test of the predictions of quantum mechanics. The experiment shows these to be accurate to a high degree of precision.

The following version of the GHZ experiment is due to Mermin [13]. Consider three spin-1/2 particles prepared in the state

$$|\psi\rangle = \frac{1}{\sqrt{2}} (|+++ \rangle - |-- \rangle) , \quad (1)$$

where $|+\rangle$ represents “up” along the z -axis and $|-\rangle$ signifies “down” along the z -axis. Now consider the results of the following products of spin measurements, each made on state $|\psi\rangle$:

(i) particle (1) along x , particle (2) along y , and particle (3) along y . Note that since $\sigma_x^1 \sigma_y^2 \sigma_y^3 |\psi\rangle = +|\psi\rangle$, the product of the results of these measurements should be $+1$, where $+1$ corresponds to the result $|+\rangle$, and -1 corresponds to $|-\rangle$.

(ii) particle (1) along y , particle (2) along x , and particle (3) along y . As in scenario (i), since $\sigma_y^1 \sigma_x^2 \sigma_y^3 |\psi\rangle = +|\psi\rangle$, the product of these results should be $+1$.

(iii) particle (1) along y , particle (2) along y , and particle (3) along x . Again, since $\sigma_y^1 \sigma_y^2 \sigma_x^3 |\psi\rangle = +|\psi\rangle$, the product of these results should also be $+1$.

(iv) particle (1) along x , particle (2) along x , and particle (3) along x . In this case, there is a significant sign difference: $\sigma_x^1 \sigma_x^2 \sigma_x^3 |\psi\rangle = -|\psi\rangle$, so the product of the results should be -1 .

The minus sign in the final scenario is crucial for differentiating between quantum mechanical and classical (*i.e.* hidden-variable) descriptions of reality. No classical hidden-variable model that assigns a classical variable (such as $+1$ or -1) to the measurement of each individual particle’s spin along axes x and y could reproduce the quantum predictions: classically, the product of the four scenarios above for a hidden-variable model must yield $+1$ because each particle is measured along each of the two axes exactly twice.

In addition to demonstrating purely quantum correlations that have no classical analog, the above set of measurements has the potential to verify the hallmark of quantum “weirdness”: non-locality. The GHZ experiment—as originally conceived—requires that the measuring apparatuses for the three particles be sufficiently distant from each other so as to eliminate the possibility of local, classical interactions between measurements that might duplicate the quantum mechanical predictions. In NMR experiments, the effective distances between any three spins in a molecule are typically a few angstroms at most; as such, it is practically impossible to demonstrate non-local effects using NMR. However, in the NMR experiment below, the system’s Hamiltonian is well known to a high degree of accuracy; thus, the NMR experiment can rule out any *standard* local interaction as the cause of the non-classical correlations.

This paper reports on the first experimental demonstration of GHZ correlations using effective pure states. Techniques now exist whereby it is possible to create an *effective* pure state in a liquid

sample of $\mathcal{O}(N_A)$ essentially non-interacting molecules at room temperature, meaning that the state of the ensemble can be described by a density matrix whose deviation from unity transforms under unitary operations exactly as a pure state density matrix. Since only the deviation density matrix (ρ), averaged over the whole sample, contains observable magnetization, quantum mechanics predicts that the results obtained from performing unitary transformations on a pseudo-pure NMR state are identical to those that would be found were one to perform the same operations on a single quantum system. For example, the same unitary operator (*e.g.*, $\mathcal{U} = e^{i\frac{\pi}{4}\sigma_x^1\sigma_x^2\sigma_x^3}$) that transforms a pure state (*e.g.*, $|+++ \rangle$) into a GHZ state (*e.g.*, $|\psi\rangle$) also transforms the deviation density matrix of an ensemble pseudo-pure state into a density matrix with the identical, non-classical correlations.

It is important to keep in mind that although the density matrix for an ensemble in an effective pure GHZ state is the same as the density matrix for an ensemble in which some fraction of the systems are in a pure GHZ state and the remainder are in a completely mixed state, these two ensembles are not the same. Two different ensembles may have the same density matrix. In the ensemble constructed here, each of the systems is in a unitarily-transformed version of a thermal state; none are in GHZ states. Nevertheless, since two ensembles with the same density matrix are indistinguishable with respect to measurement, the effective GHZ state constructed is just as effective as an actual GHZ state for testing the predictions of quantum mechanics.

Our verification of GHZ correlations was performed on a Bruker AMX400 spectrometer at room temperature. At this temperature, the Boltzmann distribution over an ensemble of homonuclear spins in a liquid NMR sample gives the average density matrix (per molecule) approximately proportional to $\mathbf{1} + \sum_j \beta_j \sigma_z^j$, where $\beta_j = 2\mu_j \mathcal{B}/k_B T = h\omega_j/k_B T \approx h\omega/k_B T \approx \beta$ is the Boltzmann factor for the j 'th spin. With $\omega \approx 100$ MHz for ^{13}C in a static magnetic field of $\mathcal{B} = 9.6$ Tesla, the room-temperature ($T \approx 300$ K) Boltzmann factor is of order 10^{-6} . Higher order terms in the density matrix expansion are at least of order 10^{-12} , and can therefore be neglected. Only the deviation of the density matrix from unity, rescaled in the rest of this paper (at equilibrium, $\rho_{eq} = \sum \sigma_z^j$), represents surplus or deficit populations in energy levels whose transitions are observable in NMR.

In our experimental setup, one set of coils was available to provide a gradient in \mathcal{B}_z across the sample. The result of a gradient is to introduce phase variations in the sample that vary spatially, which, when averaged over the whole sample, represent non-unitary operations on the ensemble density matrix. In addition, another set of coils in the $x - y$ plane can provide rf pulses that cause nearly unitary rotations of the density matrix. The rf coils are also used as pick-up coils to measure magnetization in the $x - y$ plane. For three spins (as in the demonstration below), the observable magnetization is the spatially-averaged signal during NMR signal acquisition that is proportional to $\text{tr} \left[\rho \sum \left(\sigma_x^j + i\sigma_y^j \right) \right]$. Other elements of the density matrix are unobserved. Correlations between spins can be read directly from the spectra produced by plotting the Fourier transform of the induction signal.

The sample used in the demonstration of GHZ correlations was triply-labeled (^{13}C) alanine with ^1H decoupling. The lowest-order terms in the natural Hamiltonian for the system are

$$\mathcal{H} \approx \frac{1}{2}\omega_1\sigma_z^1 + \frac{1}{2}\omega_2\sigma_z^2 + \frac{1}{2}\omega_3\sigma_z^3 + \frac{\pi}{2}J_{12}\sigma_z^1\sigma_z^2 + \frac{\pi}{2}J_{23}\sigma_z^2\sigma_z^3 \quad (2)$$

where ω_j is the Larmor precession frequency (including the effects of chemical shift) for spin j , and where J_{jk} is the usual scalar (weak) coupling between spins j and k . The strengths of the coupling interactions between the carbon spins in alanine are $J_{12} = 53.4$ Hz and $J_{23} = 35.3$ Hz. The scalar interaction between spins 1 and 3 is small ($J_{13} = 1.4$ Hz); this term and all other interactions in the Hamiltonian (including the effects of diffusion and relaxation) can be neglected over the ≈ 160 ms during which the entire experiment takes place.

The experiment works as follows:

(A) *Equilibration.* The sample is allowed to come to thermal equilibrium, in which the density matrix is:

$$\rho_{eq} = \sigma_z^1 + \sigma_z^2 + \sigma_z^3 = \begin{pmatrix} 3 & 0 & 0 & 0 & 0 & 0 & 0 & 0 \\ 0 & 1 & 0 & 0 & 0 & 0 & 0 & 0 \\ 0 & 0 & 1 & 0 & 0 & 0 & 0 & 0 \\ 0 & 0 & 0 & -1 & 0 & 0 & 0 & 0 \\ 0 & 0 & 0 & 0 & 1 & 0 & 0 & 0 \\ 0 & 0 & 0 & 0 & 0 & -1 & 0 & 0 \\ 0 & 0 & 0 & 0 & 0 & 0 & -1 & 0 \\ 0 & 0 & 0 & 0 & 0 & 0 & 0 & -3 \end{pmatrix}. \quad (3)$$

(B) *Preparation.* The sample is prepared in an incoherent mixture of two pseudopure states using the following operations:

$$\begin{aligned} \rho_{eq} \longrightarrow & \left[\frac{\pi}{2} \right]_{90^\circ}^2 - \left[\frac{\partial \mathcal{B}_z}{\partial z} \right] \\ & - \left[\frac{\pi}{2} \right]_{-90^\circ}^3 - \left[\frac{1}{4J_{23}} \right] - \left[\frac{\pi}{2} \right]_{135^\circ}^3 - \left[\frac{\partial \mathcal{B}_z}{\partial y} \right] \\ & - \left[\frac{\pi}{2} \right]_{-90^\circ}^1 - \left[\frac{1}{4J_{12}} \right] - \left[\frac{\pi}{2} \right]_{135^\circ}^1 - \left[\frac{\partial \mathcal{B}_z}{\partial x} \right] \\ & - \left[\frac{\pi}{2} \right]_{0^\circ}^2 - \left[\frac{1}{2J_{12}} \right] - \left[\frac{\pi}{2} \right]_{-90^\circ}^2 \longrightarrow \rho_{pp}. \end{aligned}$$

In this notation, each bracketed expression represents one matrix operation. Brackets containing angles indicate an rf pulse that selectively rotates the superscripted spin by the specified angle, where the subscripted “phase” designates the axis of rotation in the $x - y$ plane of the co-rotating frame. Selective pulses in this experiment required a pulse length of 2 ms. Brackets with partial derivatives indicate an applied gradient in the magnetic field along the direction in the denominator. Brackets containing a coupling constant indicate free evolution of the system under the natural Hamiltonian for the time indicated; this evolution allows the pertinent scalar coupling term to correlate spins. Pulses for refocussing or for averaging to zero other coupling terms in the natural Hamiltonian are not shown.

The result of the preparation sequence is the density matrix:

$$\rho_{pp} = \begin{pmatrix} 1 & 0 & 0 & 0 & 0 & 0 & 0 & 0 \\ 0 & 0 & 0 & 0 & 0 & 0 & 0 & 0 \\ 0 & 0 & 0 & 0 & 0 & 0 & 0 & 0 \\ 0 & 0 & 0 & 0 & 0 & 0 & 0 & 0 \\ 0 & 0 & 0 & 0 & 0 & 0 & 0 & 0 \\ 0 & 0 & 0 & 0 & 0 & 0 & 0 & 0 \\ 0 & 0 & 0 & 0 & 0 & 0 & 0 & 0 \\ 0 & 0 & 0 & 0 & 0 & 0 & 0 & -1 \end{pmatrix}, \quad (4)$$

which transforms like a balanced mixture of two pseudopure states,

$$\frac{1}{2} (|+++ \rangle \langle +++| - |-- - \rangle \langle -- -|). \quad (5)$$

(C) *Rotation.* The density matrix for the sample is now rotated via unitary operator $e^{i\frac{\pi}{4}\sigma_x^1\sigma_x^2\sigma_y^3}$ using the sequence:

$$\rho_{pp} \longrightarrow \left[\frac{\pi}{2}\right]_{-90^\circ}^1 - \left[\frac{1}{2J_{12}}\right] - \left[\frac{\pi}{2}\right]_{0^\circ}^{2,3} - \left[\frac{1}{2J_{23}}\right] - \left[\frac{\pi}{2}\right]_{180^\circ}^{2,3} - \left[\frac{1}{2J_{12}}\right] - \left[\frac{\pi}{2}\right]_{-90^\circ}^1 \longrightarrow \rho_{GHZ} .$$

The density matrix thus rotated becomes

$$\rho_{GHZ} = \begin{pmatrix} 0 & 0 & 0 & 0 & 0 & 0 & 0 & -1 \\ 0 & 0 & 0 & 0 & 0 & 0 & 0 & 0 \\ 0 & 0 & 0 & 0 & 0 & 0 & 0 & 0 \\ 0 & 0 & 0 & 0 & 0 & 0 & 0 & 0 \\ 0 & 0 & 0 & 0 & 0 & 0 & 0 & 0 \\ 0 & 0 & 0 & 0 & 0 & 0 & 0 & 0 \\ 0 & 0 & 0 & 0 & 0 & 0 & 0 & 0 \\ -1 & 0 & 0 & 0 & 0 & 0 & 0 & 0 \end{pmatrix} . \quad (6)$$

Note that this matrix has the identical off-diagonal structure as the density matrix formed from the pure state of Eq. 1:

$$\rho_{GHZ} = \frac{1}{2} (-|++\rangle\langle---| - |--\rangle\langle+++|) . \quad (7)$$

i.e., the NMR sample as prepared above represents the same quantum correlations that would be present in a pure, three-particle GHZ state.

(D) *Measurement.* An NMR measurement that demonstrates one of the $(\sigma_x^1\sigma_y^2\sigma_y^3)$, $(\sigma_y^1\sigma_x^2\sigma_x^3)$, $(\sigma_y^1\sigma_y^2\sigma_x^3)$, or $(\sigma_x^1\sigma_x^2\sigma_x^3)$ correlations is now performed by applying rf pulses to the sample to rotate the desired correlation into observable magnetization. Specifically, to measure $(\sigma_j^1\sigma_k^2\sigma_l^3)$, the pulse sequence

$$\rho_{GHZ} \longrightarrow \left[\frac{\pi}{2}\right]_{j-90^\circ}^1 - \left[\frac{\pi}{2}\right]_{l-90^\circ}^3$$

followed by data acquisition with the absorptive signal phased along k will reveal the magnitude and sign of the desired correlation in the spectrum on resonance with the second spin. Steps (A)~(C) of the experiment are then identically repeated three times, each with a different measurement sequence (D).

The results of the four measurements on the sample prepared in state ρ_{GHZ} are shown in Fig. 1. For example, to determine the correlations between $(\sigma_x^1\sigma_y^2\sigma_y^3)$, look at Fig. 1(a): the spectrum shows a multiplet of four lines. The frequency of each of the four lines corresponds to the resonant frequency of the second spin when the first and third spins are, respectively (from left to right): $|-\rangle_1|-\rangle_3$, $|+\rangle_1|-\rangle_3$, $|-\rangle_1|+\rangle_3$, and $|+\rangle_1|+\rangle_3$. The fact that the phase of the first line from the left is (+) confirms the GHZ correlation that when spin 1 is $|-\rangle$ along x and spin 3 is $|-\rangle$ along y , spin 2 is $|+\rangle$ along y . Similarly, the second line (from the left) shows a negative peak, confirming the correlation that when spin 1 is $|+\rangle$ along x and spin 3 is $|-\rangle$ along y , spin 2 is $|-\rangle$ along y . Likewise, the third line, with a negative peak, confirms the GHZ correlation that when spin 1 is $|-\rangle$ along x and spin 3 is $|+\rangle$ along y , spin 2 is $|-\rangle$ along y . Finally, the last line confirms the correlation that when spin 1 is $|+\rangle$ along x and spin 3 is $|+\rangle$ along y , spin 2 is $|+\rangle$ along y . Thus all four lines in Fig. 1(a) confirm that the product of the spin of particle 1 along x , particle 2 along y , and particle 3 along y yields the result +1, as in scenario (i) of the GHZ experiment explained above.

Demonstration of GHZ Correlations

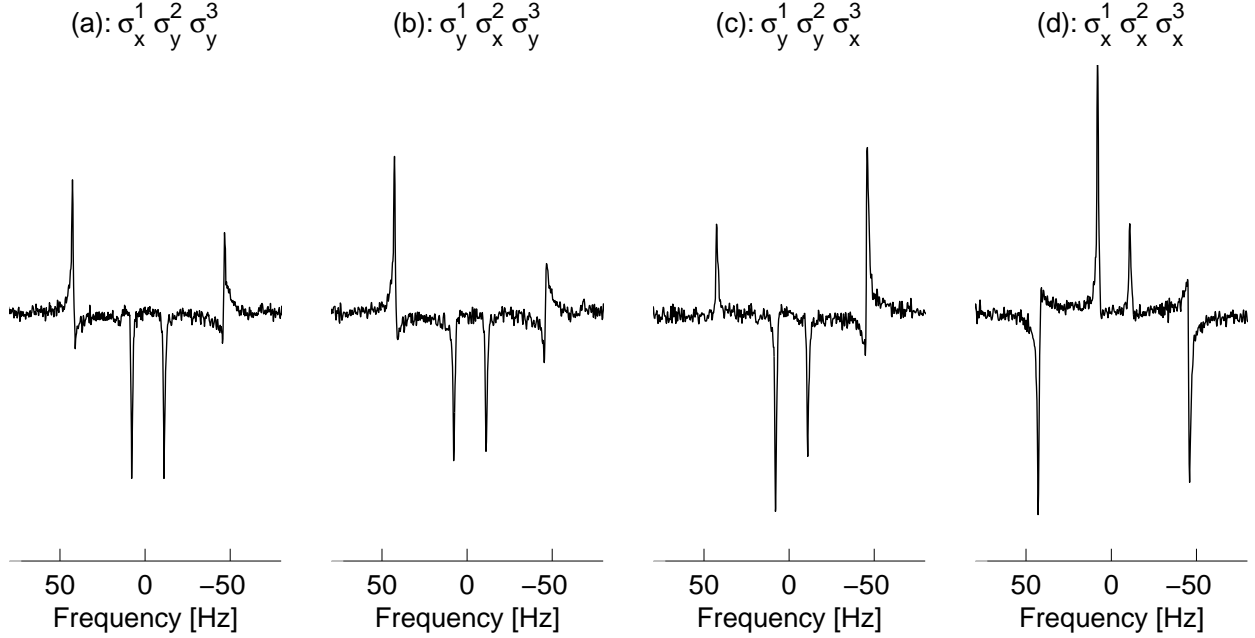


Figure 1: The confirmation of the quantum prediction of GHZ correlations. The four figures show the spectrum of spin 2 for each of the measurements. Each spectrum is split into a multiplet of four lines, corresponding to the resonant frequencies for spin 2 when spins 1 and 3 are in the states $|-\rangle_1|-\rangle_3$, $|+\rangle_1|-\rangle_3$, $|-\rangle_1|+\rangle_3$, and $|+\rangle_1|+\rangle_3$ respectively. An ‘up’ line indicates the state $|+\rangle$ for spin 2, and a ‘down’ line indicates the state $|-\rangle$. Plot (a) confirms the GHZ correlation that the product of measurements of σ_x on the first spin, σ_y on the second spin, and σ_y on the third spin yields the result +1. For example, the first line in (a) indicates that when spins 1 and 3 give the result $(-1)_1(-1)_3$, spin 2 gives the result +1; the second line indicates that when spins 1 and 3 give the result $(+1)_1(-1)_3$, spin 2 gives the result -1; *etc.*, so that the product of the results is always +1. Similarly, (b) and (c) confirm that the products $\sigma_y^1 \sigma_x^2 \sigma_y^3$ and $\sigma_y^1 \sigma_y^2 \sigma_x^3$ also yield the result +1. Plot (d), by contrast, shows that the product $\sigma_x^1 \sigma_x^2 \sigma_x^3$ yields the result -1, in contradiction to the predictions of the classical hidden variable theory.

Note that Fig. 1(b) shows the same four lines in the spectrum for spin 2, except that in this case the measurement sequence reveals the correlation that corresponds to $\sigma_y^1 \sigma_x^2 \sigma_y^3$. As in Fig. 1(a), all four lines indicate that the product of the spin of particle 1 along y , particle 2 along x , and particle 3 along y is +1, as predicted in scenario (ii) above. Likewise, Fig. 1(c) shows the analogous +1 result when the product of spin measurements of particle 1 along y , particle 2 along y , and particle 3 along x is computed.

Significantly, Fig. 1(d) shows a different spectrum when a measurement of the correlation ($\sigma_x^1 \sigma_x^2 \sigma_x^3$) was made. In this case, when spin 1 is $|-\rangle$ along x and spin 3 is $|-\rangle$ along x , spin 2 is $|-\rangle$ along x , as seen in the first line; when spin 1 is $|+\rangle$ along x and spin 3 is $|-\rangle$ along x , spin 2 is $|+\rangle$ along x ; and so forth. In this case, the product of the spin measurements of particle 1 along x , particle 2 along x , and particle 3 along x is *not* +1, but rather -1 . Taken together, the four spectra in Fig. 1 clearly demonstrate the GHZ correlations predicted by quantum mechanics.

Although the NMR experiment demonstrates GHZ correlations, it cannot eliminate local interactions as the cause of those correlations because of the close proximity of the nuclei involved. However, no known interaction in the natural Hamiltonian could be responsible for the “communication” between the nuclei that caused the GHZ correlations. Specifically, measurement step (D) required only 4.043 ms to implement; this represents the amount of time *after* the GHZ preparation steps (A)~(C)—common to all four experiments—but before data acquisition, in which the culpable classical local interaction could “inform” the spins of which axes were being measured for which spins and then adjust the phase of the acquisition signal to reveal the quantum mechanical correlations. Since the fastest coupling term in the natural Hamiltonian is slower than 4.043 ms ($1/2J_{12} = 9.36$ ms), the culpable “classical demon,” if it exists, would have to be a non-standard interaction.

In addition, the NMR experiment cannot completely rule out classical hidden variables. The effective pure state used to demonstrate GHZ correlations is in fact a mixed state of an ensemble in which individual members are unitarily transformed from a thermal state. It can be shown that such states can be described by non-negative discrete Wigner functions[16, 17]. Accordingly, the results of the experiment could be “explained” by a hypothetical ensemble of classical systems each of which possesses a definite state for its hidden variables. As in the case of local interactions in the previous paragraph, however, to be consistent with the measured properties of the states (3-5) above the preparation of such an ensemble from the thermal ensemble with which the experiment begins would require a conspiracy of non-standard interactions.

In conclusion, this paper reported on an experiment that displays GHZ correlations using nuclear magnetic resonance. Although the NMR experiment performed cannot entirely rule out classical local hidden variables, it nonetheless provides an unambiguous and statistically significant demonstration of the apparently paradoxical GHZ correlations. In addition, the experimental demonstration of GHZ correlations using NMR underscores the ability of NMR to perform significant experiments in fundamental quantum mechanics.

Acknowledgements: This work was supported by DARPA.

References

- [1] A. Einstein, B. Podolsky, and N. Rosen, Can quantum- mechanical description of reality be considered complete?, *Phys. Rev.* 47:777-780 (1935).
- [2] D. Bohm, *Quantum Theory*, Prentice-Hall: Englewood Cliffs (1951).
- [3] D. Bohm, A suggested interpretation of the quantum theory in terms of “hidden” variables, I and II, *Phys. Rev.*, 85:166-179 (1952).
- [4] J. Bell, On the Einstein Podolsky Rosen paradox, *Physics* 1:195-200 (1964).
- [5] A. Aspect, P. Grangier, and G. Roger, Experimental tests of realistic local theories via Bell’s theorem, *Phys. Rev. Lett.*, 47:460-463 (1981).
- [6] A. Aspect, P. Grangier, and G. Roger, Experimental realization of Einstein-Podolsky-Rosen-Bohm gedankenexperiment: a new violation of Bell’s inequalities, *Phys. Rev. Lett.*, 49:91-94 (1982).
- [7] D. Greenberger, M. Horne, A. Shimony, and A. Zeilinger, Bell’s theorem without inequalities, *Am. J. Phys.*, 58:1131-1143 (1990).
- [8] N. Gershenfeld and I. Chuang, Bulk spin-resonance quantum computation, *Science*, 275:350-356 (1997).
- [9] D. Cory, A. Fahmi, and T. Havel, Ensemble quantum computing by nuclear magnetic resonance spectroscopy, *Proc. Natl. Acad. Sci.* 94:1634-1639, 1997.
- [10] D. Cory, M. Price, and T. Havel, Nuclear magnetic resonance: an experimentally accessible paradigm for quantum computing, *Physica D*, 120:82-101 (1998).
- [11] S. Lloyd, Microscopic analogs of the Greengerger-Horne- Zeilinger experiment, *Phys. Rev. A*, 57:R1473-R1476 (1998).
- [12] R. Laflamme, E. Knill, W. Zurek, P. Catasti, and S. Mariappan, NMR GHZ, *Phil. Trans. Roy. Soc. Lond.*, A356:1941-1948 (1998).
- [13] N. Mermin, Quantum mysteries revisited, *Am. J. Phys.*, 58:731-734 (1990).
- [14] C. Bennett, D. DiVincenzo, J. Smolin, and W. Wootters, Mixed-state entanglement and quantum error correction, *Phys. Rev. A* 54:3824-3851 (1996).
- [15] J. Schlienz and G. Mahler, Description of entanglement, *Phys. Rev. A* 52:4396-4404 (1995).
- [16] S. Lloyd, Discrete Wigner Functions, in preparation.
- [17] S.L. Braunstein, *et al.*, Separability of very noisy mixed states and implications for NMR quantum computing, *quant-ph/9811018* (1998).